G. D. Martin, J. R. Castrejon-Pita and I. M. Hutchings, in Proc 27th Int. Conf. on Digital Printing Technologies, NIP27, Minneapolis, MN, USA, 2011 620-623, 'Holographic Measurement of Drop-on-Demand Drops in Flight'.

Holographic Measurement of Drop-on-Demand Drops in Flight

Journal:	*NIP and Digital Fabrication 2011*
Manuscript ID:	74
Presentation Type:	Oral
Date Submitted by the Author:	05-Jul-2011
Complete List of Authors:	Martin, Graham; University of Cambridge, Engineering Castrejon-Pita, Jose Rafael; University of Cambridge Hutchings, Ian; University of Cambridge, Engineering

Holographic Measurement of Drop-on-Demand Drops in Flight

Graham D. Martin, José R. Castrejón-Pita and Ian M. Hutchings; Institute for Manufacturing, University of Cambridge, UK

Abstract

The analysis of images of ink drops in flight can provide information about jet straightness, drop velocity and volume. However trade-offs between field of view, optical and digital resolution and other factors such as depth of field and optical distortion, limit the accuracy and amount of information available from a single image. In-line, digital holograms of drops in flight can capture information from fields of view at least as large as the area of the digital sensor. Using mathematical reconstruction techniques particularly suited to sparse, small objects of regular geometry the accuracy of measurement can potentially be sub-micrometer on drop position and diameter.

This paper describes our experimental apparatus, hologram reconstruction techniques and the results of experiments on imaging drops. We also discuss techniques to improve the accuracy of the technique in the direction of the optical axis.

Introduction

Drop-on-demand (DoD) inkjet printers are used for high resolution imaging and, increasingly for digital fabrication. These applications demand high drop placement accuracy and, in some cases, precise control over drop volume. Accurate measurement of drop direction, velocity and volume is therefore required.

Existing techniques include taking optical shadowgraph images at some suitable magnification [1]. To obtain enough resolution to measure precisely, high magnifications are required and hence fields of view are restricted to one or a few drops. At lower magnifications more drops can be seen but the digital resolution is too low to measure position accurately. For example, because the pixels on photographic image sensors are typically 5 to 10 µm square, at a magnification producing life size images on the camera sensor (ie 1:1 macro) a single drop is only a few pixels in diameter making accurate position and volume measurement impossible. Even at high magnifications problems such as limited depth of field, optical lens distortions and thresholding issues can limit the measurement accuracy and introduce systematic errors.

Drop volumes are particularly subject to error when measured optically as only the drop diameter can be measured. Other techniques have been employed. For example, Verkouteren [2] weighed large numbers of drops which can give an accurate mean value but cannot study drop to drop variation easily. It is possible to imagine using other techniques such as quartz crystal resonators and micro-cantilevers [2].

Holography is a technique in which the interference pattern created by the interaction of coherent light scattered from an object and a reference beam from the same source is recorded on film or, more recently, on a digital photographic sensor. Optical reconstruction of film-based holograms is achieved by diffracting a beam, like the reference beam, through the film, producing a 3-dimensional image. Digitally captured holograms make possible mathematical reconstruction of an image which can then be processed digitally or used to generate visible images [3].

In-line digital holography [4] is a simple technique applicable when objects are small and sparse. In this case a single collimated laser beam is used to illuminate the objects and then both the light scattered by the objects and the unaffected beam are captured by an exposed digital image sensor which records the interference between the scattered and unscattered light. Hence the beam acts as both illumination and reference.

By using appropriate mathematical reconstruction techniques (see below), the position (in 3 dimensions) and size of objects within the field of view (ie the size of the image sensor) can be estimated to micrometer accuracy. If we know that the objects are spherical then we can use that knowledge to employ methods that can improve the measurement accuracy to significantly better than 1 µm. If the illumination is larger than the sensor area, then even objects outside the geometrical field of view implied by the sensor size can be reconstructed, as the sensor will capture the interference patterns of light scattered from them.

Experimental apparatus

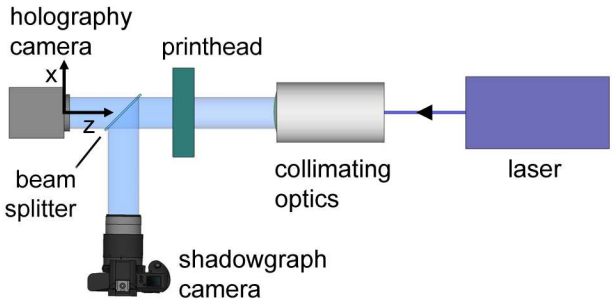

Figure 1. *Apparatus.*

Figure 1 illustrates the experimental arrangement. An Oxford Lasers Nd:YAG laser with a frequency doubled beam having a wavelength of 532 nm and a short duration pulse (~5 ns) was used, with appropriate optics, to produce a collimated beam approximately 20 mm in diameter. This beam passes through the object area and then falls directly onto an exposed digital sensor (JAI RM-2040GE, 1600 x 1200 pixels) without any further intervening optics. If the laser is coherent enough then the light scattered by the objects will create an interference pattern which can be recorded by the digital sensor.

In some experiments a half-silvered mirror was inserted as a beam-splitter between the objects and the sensor so that some of the light was diverted to a camera (Nikon D80) with a lens (Tamron SP AF 90mm F/2.8 Di Macro) focused on the objects such that the image created was a 1:1 macro image of the objects. Hence the field of view of the macro image formed by the lens was very similar to the field of view of the holography sensor.

The printhead used during these experiments was the Dimatix SE-128, drop-on-demand, inkjet printhead. Timing equipment, not shown in figure 1, was used to synchronize the firing of the drops, the activation of the camera sensor and the pulsing of the laser such that images and interference patterns produced by drops in-flight were recorded.

Reconstruction techniques

Several techniques exist to mathematically reconstruct the image associated with a digital hologram. In this work we used the diffraction integral, transfer function (DITF) method described in Kreis et al. [5] to initially locate ink drops in the image and then the inverse-problem (IP) approach described by Soulez et al. [6] and Gire et al. [7] to refine the location measurement. The initial reconstruction is based on solving the Rayleigh-Sommerfeld diffraction formula [8]. The DITF approach results in an algorithm involving a Fourier transform and an inverse Fourier transform of the form:

$$W = |F^{-1}\{F\{H \cdot R\} \cdot G\}|^2 \quad (1)$$

$$G = f(x,y,z,\lambda) \quad (2)$$

where W is the reconstructed image of the hologram H, R represents the reference wave field (in this case a constant) and G is a transfer function involving only the location of the pixels to be reconstructed and the wavelength, λ, of the light used. The DITF algorithm, the IP algorithm described below and other functions were implemented in a Matlab program.

In the holograms taken during the experiments described below it was found that there were significant amounts of unwanted patterns arising from, for example, dust on optical elements, edges such as the edge of the printhead and from interference patterns arising from optical elements (for example the sensor protective cover). It was found to be advantageous to take a background image, containing no printed drops, soon before or soon after the image captured from drops in flight. This background image is subtracted from the hologram before reconstruction, removing many of the unwanted elements.

The next step is to perform the calculation summarized in equation (1) at appropriate z locations through the image. In this way a 3-dimensional representation of the region containing the drops is reconstructed. Image analysis techniques similar to those used to find objects in 2-D images are used to find objects in this 3-D space. Estimates of location and size of these objects can be made. Tests with simulated holograms (see below) indicate that this technique, using the geometry and typical drop sizes of our experiments, can estimate the x, y location and drop diameter to an accuracy of a few micrometers. The estimate of the z location (ie the direction along the optical axis) was about two orders of magnitude worse. While this accuracy is sufficient for some purposes (particularly considering the large field of view) it is not good enough for experimentally investigating changes in drop direction and velocity and particularly drop volume.

The inverse-problem approach is a method which can potentially improve the accuracy of the measurement. In this technique it is assumed that the drops are spherical. If the approximate location and size of a drop is known then a simulated hologram can be constructed and the difference calculated between the real and simulated hologram.

It is possible to construct a simulated hologram as it can be shown [7] that a spherical object will produce a pattern on the sensor closely following:

$$g(x,y) = \frac{\pi r^2}{\lambda z} J\left(\frac{2\pi r\sqrt{x^2+y^2}}{\lambda z}\right)\sin\left(\frac{\pi\left(x^2+y^2\right)}{\lambda z}\right) \quad (3)$$

Where J is defined by:

$$J(a) = \frac{J_1(a)}{a} \quad (4)$$

here $g(x, y)$ is the intensity variation of a hologram centered at x=y=0, J_1 is a Bessel function of the first kind and order 1, x and y are the coordinates from the centre of the hologram, z is the distance from the hologram to the object, r is the diameter of the sphere and λ is the wavelength of the light.

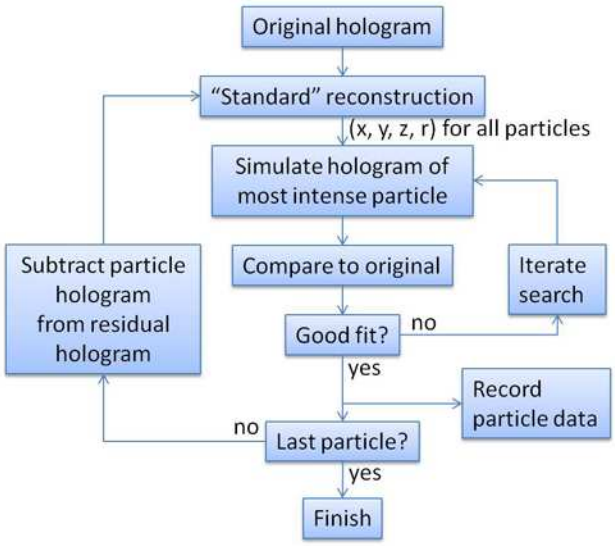

Figure 2. *Flow diagram of the iterative calculation method.*

Bu using appropriate iterative searching techniques the position and size of the drop creating the simulated hologram are adjusted until the simulation matches the real hologram to within a set amount. In the Matlab program the DITF method ("standard" reconstruction) is applied to the hologram, the largest drop is selected and the IP process is used to refine the drop parameters. The simulated hologram is then subtracted from the real hologram and the calculation is iterated until all of the drops have been processed. Figure 2 shows a flow diagram of the iterative technique used.

Determining when the last particle has been processed can be a problem as the algorithm will continue to attempt to find particles and may process noise or the "ghost" patterns left after particle subtraction. If the exact number of particles is not known

then estimates of signal-to-noise ratios or particle coincidence (from the ghost patterns) can be used to halt the process.

Tests, Experiments and Results

To test the algorithms a simulated hologram was constructed with 4 spherical "drops" of known location and size, using the techniques described above (figure 3(a)). Initially the DITF technique was used alone to estimate the drop parameters. The differences between these estimates and the actual values are listed in table 1. The hologram was then re-evaluated using the full DITF+IP process and the results from this are also listed in Table 1 where the figures presented show the absolute difference between the calculated value and the actual value. For each of *x*, *y*, *z* and *r* the figures are the mean of the values for all four drops (this is a similar calculation to that described by equation (5) below).

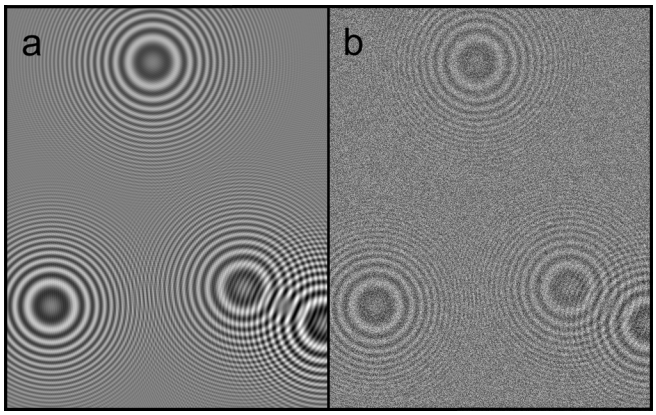

Figure 3. *(a) Simulated hologram. (b) With reduced contrast and added noise.*

To evaluate the sensitivity of the algorithms to image contrast and noise the simulated hologram was also degraded by reducing its contrast (Photoshop CS4 > image adjustments > levels) to 40% of the original value and introducing 10% noise (Photoshop CS4 > filter > noise > add noise). The resulting image is shown in Figure 3(b) and the results of estimating the drop parameters are listed in Table 1.

Table 1. Results of tests on the simulated hologram: errors in *x*, *y*, *z* and *r*.

process	***x***	***y***	***z***	***r***
	µm	***µm***	***µm***	***µm***
DITF only	*0.278*	*0.907*	*467.500*	*29.730*
DITF+IP	*0.042*	*0.120*	*7.238*	*0.060*
degraded	*0.128*	*0.178*	*11.844*	*0.462*

These results indicate that while using the DITF process alone produces a reasonable result for *x* and *y*, the *z* and *r* values are poor although it might be possible to improve the r value by improving image processing techniques. Using the combined DITF and IP processes shows a significant improvement in parameter estimation, over 60 times for the *z* estimate and nearly 500 times better for the estimate of radius. The estimates of parameters for the degraded images show a reduced correspondence with the original but still good enough for useful measurements except in the case of the along the optical axis measurement (*z*). Means to improve this measurement are discussed below.

Using the apparatus described above, a series of hologram and shadowgraph pairs were captured of drops in flight. These drops were nominally 15 µm in radius and were travelling at a velocity of 5 ms^{-1}.

Figure 4 shows details from larger images and includes both holographic and shadowgraph images of these real ink drops in flight. Figure 4(a) is part of the hologram showing four patterns out of the 12 drops captured in total, 4(b) is the same area of the hologram with the background subtracted, 4(c) is the shadowgraph taken at the same time and of the same area as 4(a), and 4(d) is one of the reconstructed image slices which are part of the outputs of the DITF process showing white drop images on a black background. From the set of reconstructed slices like 4(d) an estimate of the drop positions can be made and used as the starting point for the IP process. A blow-up of the shadowgraph image of the upper drop is inserted in figure 4(c). The drop image is only about 6 pixels across and as this is a 1-to-1 macro image and the pixels are 7.4 µm square then clearly estimating position or radius to better than O(10 µm) would be difficult.

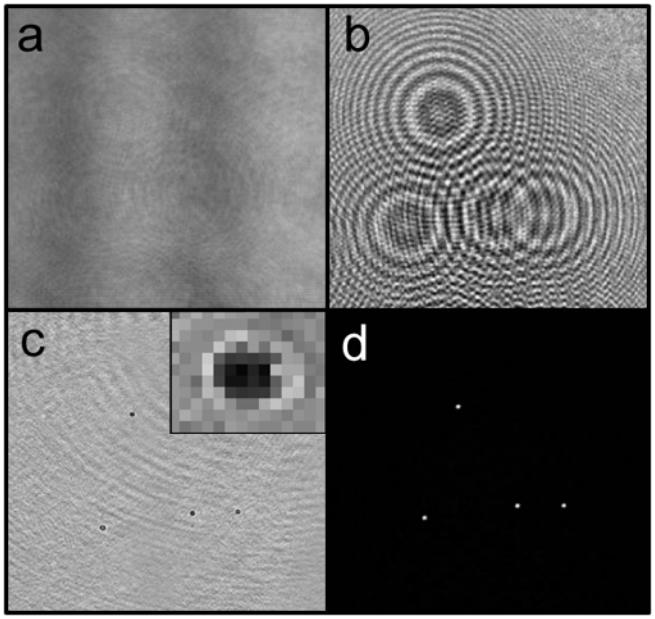

Figure 4. *(a) region of hologram, (b)after background subtraction, (c) shadowgraph and (d) DITF reconstruction.*

Figure 5(a) shows a larger area of the original hologram shown in figure 4. Here all of the patterns associated with the 12 drops are displayed. This is the hologram after a background image, taken following the hologram capture, had been subtracted from the original image. This image was processed using the DITF + IP process described above. As explained, after each drop is evaluated the best calculated holographic pattern is subtracted from the image before the process addresses the next drop. Figure 5(b) shows the image after the sixth drop to be processed has been subtracted. At this point the adjusted image would be evaluated using DITF and the new "largest" drop chosen and its parameters

refined by the IP process. This then continues until no holographic patterns associated with drops remain in the image.

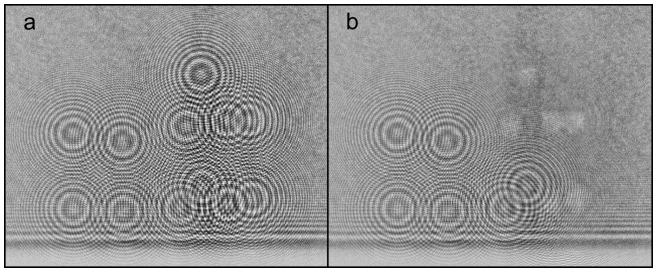

Figure 5. *(a) Hologram before processing, (b) after six drops have been processed.*

To evaluate how robust the process is to background noise the same holographic image described above was reprocessed but this time with a different background image (the one taken before the hologram) subtracted. This resulted in significantly different noise patterns in the image to be processed. The results of processing these two images are listed in table 2.

Table 2. Variation with background noise: changes to coordinates resulting from the use of different background holograms.

x	*y*	*z*	*r*
µm	*µm*	*µm*	*µm*
0.036	*0.087*	*36.577*	*0.206*

Table 2 shows the absolute difference between the measurements of each drop's parameters made with each background averaged over the 12 drops as shown for x in equation (5) where xa_n and xb_n are the measured x locations of the n^{th} drop in each of the two images created by subtracting the different backgrounds.

$$x = \frac{\sum_{n=1}^{n=12} \left| xa_n - xb_n \right|}{12} \tag{5}$$

These results indicate that the x, y and r are potentially sub-micrometer in accuracy while the z measurement is not.

Conclusions and future work

The results presented here suggest that high resolution estimates of drops positions (x, y) and radius (r) can be made over large fields of view (and potentially beyond, given that interference patterns associated with drops beyond the field of view will still be apparent). Unfortunately the accuracy obtained for the positions along the optical axis (z) does not seem to be good enough (for estimating jet direction for example). Figure 6 shows a proposed experimental arrangement which could overcome this limitation and also, because the print head would be placed at 45° to the optical axes, could include more drops in the field of view.

In this arrangement the half silvered and full mirrors are used to split the laser beam so that two images are captured at the same moment with perpendicular views of the ink drops hence removing the need to rely on the z measurement in either view. It may be necessary that the path length difference between the optical paths is greater than the coherence length of the laser to avoid unwanted interference between the light in the two paths.

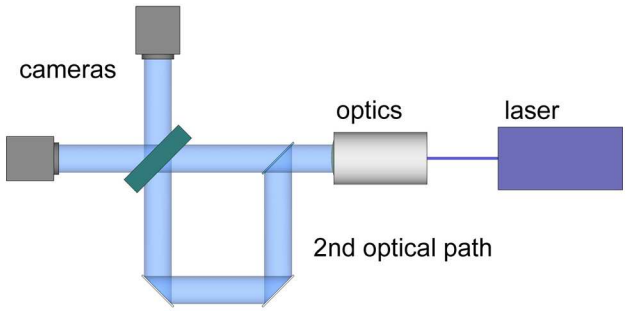

Figure 6. *Proposed arrangement to improve z resolution.*

Acknowledgements

This work was supported by the UK Engineering and Physical Sciences Research Council (project: EP/H018913/1) and by a consortium of industrial partners.

References

[1] I.M. Hutchings, G.D. Martin, and S.D. Hoath, "High speed imaging and analysis of jet and drop formation," *Journal of Imaging Science and Technology*, vol. 51, 2007, p. 438.

[2] R.M. Verkouteren and J.R. Verkouteren, "Inkjet metrology: high-accuracy mass measurements of microdroplets produced by a drop-on-demand dispenser.," *Analytical chemistry*, vol. 81, Oct. 2009, pp. 8577-84.

[3] J. Katz and J. Sheng, "Applications of Holography in Fluid Mechanics and Particle Dynamics," *Annual Review of Fluid Mechanics*, vol. 42, Jan. 2010, pp. 531-555.

[4] J.P. Fugal, T.J. Schulz, and R. a Shaw, "Practical methods for automated reconstruction and characterization of particles in digital in-line holograms," *Measurement Science and Technology*, vol. 20, Jul. 2009, p. 075501.

[5] T.M. Kreis, M. Adams, and W.P.O. Juptner, "Methods of digital holography: A comparison," *SPIE*, vol. 3098, 1997, pp. 224-233.

[6] F. Soulez, L. Denis, C. Fournier, E. Thiébaut, and C. Goepfert, "Inverse-problem approach for particle digital holography: accurate location based on local optimization.," *Journal of the Optical Society of America. A, Optics, image science, and vision*, vol. 24, Apr. 2007, pp. 1164-71.

[7] J. Gire, L. Denis, C. Fournier, E. Thiébaut, F. Soulez, and C. Ducottet, "Digital holography of particles: benefits of the 'inverse problem' approach," *Measurement Science and Technology*, vol. 19, Jul. 2008, p. 074005.

[8] J.W. Goodman, *Introduction to Fourier Optics 3rd Edition*, Roberts & Co, 2005.

Author Biography

Dr Graham Martin is the Director of the Inkjet Research Centre at the Institute for Manufacturing, University of Cambridge. He has a PhD in solid state physics and has worked in NIP-related research, consultancy and product development for many years. The companies he has worked for include: Cambridge Consultants Ltd (Non Impact Printing Systems group leader), Elmjet (Technical Director) and Videojet (Director of Technology).